Nitrification in the water column of Lake Erie: seasonal patterns, community dynamics, and competition with cyanoHABs

Authors: Hoffman, D.K., McCarthy, M.J., Zastepa, A., Boedecker, A.R., Myers, J.A., Newell, S.E.

ABSTRACT

This study reports directly measured nitrification rates in the water column of western Lake Erie, which is affected by annual cyanobacterial harmful algal blooms (cyanoHABs), and across all three Lake Erie basins. Over three field seasons, $^{15}NH_4^+$ stable isotope tracers were employed to quantify nitrification rates, and relative abundances of ammonia-oxidizing bacteria (AOB) and archaea (AOA) were determined via qPCR. Nitrification rates ranged from undetectable to 1,270 nmol L^{-1} d^{-1} and were generally greatest in the western basin near the Maumee River mouth (a major nutrient source). Nitrification rates were highest in early summer, and often lowest during peak cyanoHAB months (August and September), before increasing again in October. In the western basin, nitrification was negatively correlated with cyanobacteria biomass. There were no consistent differences in nitrification rates between the three Lake Erie basins. Over the three years in western Lake Erie, AOB and AOA were often present in high and similar abundances, but overall, AOB exceeded AOA, particularly in 2017. No relationships were observed between nitrification rates and AOB and AOA abundances. Thus, despite abundant ammonia-oxidizer DNA, lower nitrification rates during cyanoHABs suggest that nitrifiers were poor competitors for regenerated and available NH_4^+ during cyanoHABs, as also observed in similar systems. Low nitrification rates during cyanoHABs could limit system N removal via denitrification, a natural pathway for excess nitrogen (N) removal and a valuable ecosystem service. Lower denitrification rates allow more bioavailable N to remain in the system and support biomass and microcystin production; therefore, these results help explain how non-N-fixing cyanoHABs persist, despite low bioavailable N concentrations during cyanoHABs, and support management efforts to reduce external N loading to eutrophic systems.

Keywords: nitrogen, cyanobacteria, eutrophication, freshwater

INTRODUCTION

Lake Erie is the smallest (by volume), shallowest, and warmest of the Laurentian Great Lakes and is subject to ecological and human health concerns due to annual and seasonal harmful cyanobacterial blooms (cyanoHABs; Watson et al., 2016). The proliferation of western basin cyanoHABs in summer since the mid-1990s has been linked to complex interactions of physicochemical factors, including the availabilities of phosphorus (P; e.g., Scavia et al., 2014) and chemically reduced nitrogen (N) forms, such as ammonium (NH_4^+; Newell et al., 2019; Hoffman et al. 2022). Since the late 1980s, all three basins have been invaded by *Dreissenid* mussels (zebra and quagga; Barbiero and Tuchman, 2004), which improve water clarity but also promote cyanoHABs via rapid nutrient cycling (Conroy et al., 2005) and selective filter-feeding (Vanderploeg et al., 2001). The central basin is subject to cyanoHABs dominated by *Dolichospermum* (capable of N fixation) in June and July and non-N-fixing *Microcystis* in August and September (Chaffin et al., 2019). *Microcystis* are particularly competitive for NH_4^+ (Blomqvist et al., 1994; Monchamp et al., 2014) and may spread to or be transported into the central basin (Chaffin et al., 2019).

Nitrification is a key link between organic matter remineralization (producing NH_4^+) and N removal via denitrification (producing N_2 gas, which leaves the system). Nitrification thus helps mitigate excess N loading by producing the substrate for, and often coupling with, denitrification (e.g., Boedecker et al. 2020). In canonical nitrification, ammonia oxidation converts NH_4^+ to nitrite (NO_2^-), which is then oxidized to nitrate (NO_3^-) via NO_2^- oxidation (Prosser, 1990; Hart et al., 1994; Kuypers et al. 2018). In this two-step process, ammonia oxidation is the rate-limiting step, in which ammonia monooxygenase (encoded by the *amoA* gene) transforms NH_4^+ to an intermediate compound, hydroxylamine, which is then converted to NO_2^- (Ward, 2008). Ammonia oxidation is performed by chemolithoautotrophic

bacteria (ammonia-oxidizing bacteria, AOB; Wagner et al., 1995) and archaea (ammonia-oxidizing archaea, AOA; Francis et al., 2005). Together, they comprise the community of ammonia-oxidizing organisms (AOO). The second step of nitrification, NO_2^- oxidation, is carried out by NO_2^--oxidizing bacteria (NOB). Historically, NO_2^- oxidation has been considered separate from (although often closely linked to) ammonia oxidation, wherein the product of ammonia oxidation serves as the substrate for NO_2^- oxidation (Ward, 2008). The canonical understanding of nitrification has been updated by the discovery of certain NOB that can perform the entire nitrification pathway (complete ammonia oxidation, or comammox), and their role in the environment is still being described (Daims et al., 2015; Kuypers et al., 2018).

Nitrification links chemically reduced and oxidized N forms, and, thus, represents the link between the most favorable N form for many primary producers, including cyanoHABs (Glibert et al., 2016), and the substrate for natural N removal (via denitrification). *Microcystis* dominates cyanoHABs in western Lake Erie, cannot fix atmospheric N, and are excellent competitors for NH_4^+ (Takamura et al., 1987; Blomqvist et al., 1994; McCarthy et al. 2007); as such, they may quickly deplete bioavailable N pools. CyanoHABs in eutrophic waterbodies, such as Lake Erie, may threaten the ability of the system to compensate for excess N inputs by suppressing nitrification via substrate competition (Hampel et al., 2018). *Microcystis* in culture exhibits a half-saturation constant (K_m) related to maximum specific growth rate for NH_4^+ of 0.5–37 μM, higher than that of AOA but within the range for AOB (Nicklisch and Kohl, 1983). Therefore, AOO community structure during cyanoHABs may influence the ability of nitrifiers to compete with bloom-forming taxa for NH_4^+ and alter the fate of NH_4^+ via removal or recycling (Hampel et al., 2018, 2020).

As a result of high external nutrient loading from adjacent watersheds, Lake Erie experiences annual, seasonal cyanoHABs dominated by non-N fixing *Microcystis*, which are largely restricted to the western basin (Watson et al., 2016). Two studies have shown that AOB greatly outnumber AOA in the sediments (Bollman et al., 2014) and water column (Mukherjee et al., 2016) of Lake Erie. A previous study estimated that 96% of the N removed in Lake Erie sediments was due to coupled nitrification-denitrification (Small et al., 2014), a finding supported by subsequent work showing that NO_3^- enrichment did not stimulate direct denitrification in western basin sediments (Boedecker at al., 2020). Given high nutrient loads and the physiological importance of NH_4^+, the lack of measured nitrification rates represents a knowledge gap, particularly in freshwater eutrophic lakes.

Direct measurements of water column nitrification in lakes are few compared to rates from coastal systems and the open ocean (Damashek and Francis, 2018). Nitrification in the water column of eutrophic lakes has been quantified in Lake Taihu (Hampel et al., 2018), Lake Mendota (Hall, 1986), and Lake Okeechobee (Hampel et al., 2019, 2020). Nitrification often represented a small proportion of total microbial NH_4^+ demand in these lakes, which are all affected by cyanoHABs, indicating that nitrifiers often are not competitive for NH_4^+ during cyanoHABs. Along with nitrification rates, characterizations of the AOO community in the water column of freshwater systems is lacking compared with those from sediments in the same systems (Damashek and Francis, 2018; Hampel et al., 2020). Accordingly, there is a need to quantify both nitrification rates and the abundance of AOB and AOA in freshwater systems.

Quantifying the fate of NH_4^+ is crucial for modeling the ability of denitrification to remove excess bioavailable N from aquatic systems. Seasonally, models and incubations both show that NO_3^- limits direct denitrification in many lakes (Rissanen et al., 2013; Powers et al., 2017; Cavaliere et al., 2018), including Lake Erie (Small et al., 2016; Boedecker et al., 2020). However, many ecosystem models for Lake Erie do not include N or within-system N dynamics (e.g., Bertani et al., 2016; Scavia et al., 2023). The objective of this study was to quantify nitrification rates (as accumulation of $^{15}NO_2^-$ and $^{15}NO_3^-$ from $^{15}NH_4^+$ used as a stable isotope tracer) along seasonal and spatial gradients in Lake Erie. The abundance of *amoA* genes for AOB and AOA were determined to assess AOO community structure in the western basin. This project combined biogeochemical and molecular techniques to determine the relative contribution of nitrifiers to total community NH_4^+ demand (as reported in Hoffman et al., 2022) and the generation of substrate for denitrification. Considering the findings of previous work describing the impact of *Microcystis*-dominated cyanoHABs on nitrification in other freshwater systems, we

hypothesized that nitrification rates in Lake Erie would be highest during pre- and post-bloom sampling periods, while rates during cyanoHABs would be lower. It was also expected that AOO community abundances would be lower during peak cyanoHABs and within blooms in the western basin.

METHODS

Site description

From west to east, Lake Erie spans a length of approximately 350 km, with a coastline covering nearly four times that length (~1,400 km) and including four U.S. states (Ohio, Michigan, New York, and Pennsylvania) and one Canadian province (Ontario). Its waters represent a surface area of more than 25,000 km^2, with an estimated volume of 483 km^3 and a watershed drainage area of 78,000 km^2 (United States Environmental Protection Agency (US EPA)). This water volume is spread across three morphologically and trophically distinct basins. The western basin, eutrophic and prone to disruptive cyanoHABs, is the shallowest and most well-mixed, with an average depth of 7.4 m. The central basin is mesotrophic, experiences seasonal bottom-water hypoxia and cyanoHABs (Chaffin et al., 2019), and has an average depth of 18.3 m (PA DCNR 2010). The eastern basin is the deepest and least productive, with an average depth of 27 m (Great Lakes Fisheries Commission, 2017), and has the most oligotrophic profile in offshore regions (Edwards et al., 1990; Barbiero and Tuchman, 2004; Depew et al. 2006; Wang et al., 2008).

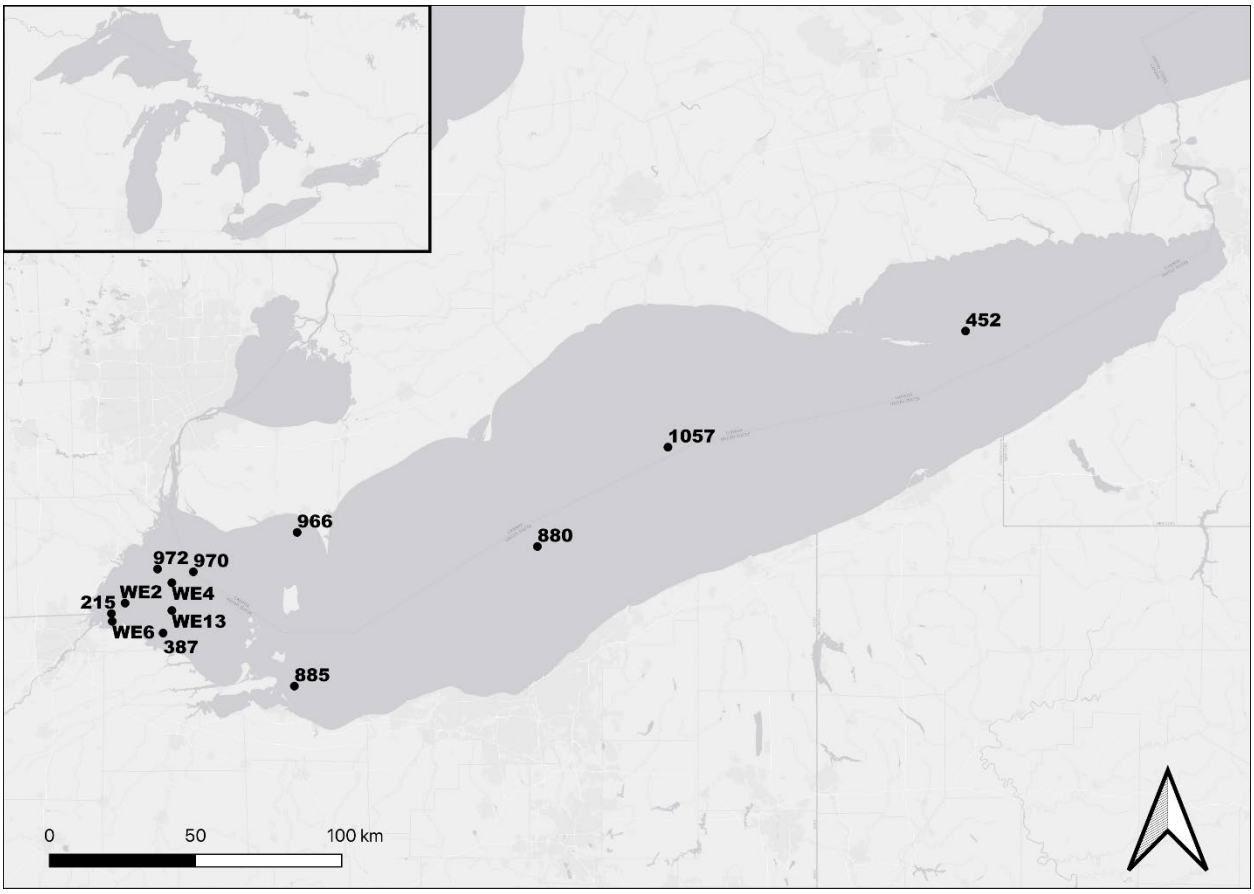

Figure 1. Sampling stations across Lake Erie. Stations WE2, WE4, WE6, and WE13 were sampled with NOAA GLERL/CIGLR. Numbered stations were sampled with Environment and Climate Change Canada (ECCC) aboard the *CCGS Limnos*.

Field sampling

Field sampling procedures, in situ water quality measurements, sampling stations, and sampling dates for nitrification rates were previously described in Hoffman et al. (2022). Briefly, water sampling in western Lake Erie was conducted monthly, during the growing season, alongside the NOAA Great Lakes Environmental Research Laboratory's (GLERL) and Cooperative Institute for Great Lake Research's (CIGLR) weekly HABs monitoring program at three or four stations at both ~1 m below the water surface and ~1 m above sediments (Fig. 1; station and month combinations varied depending on year). Ambient physicochemical parameters, including water temperature, dissolved oxygen concentration, Secchi depth, conductivity, photosynthetically active radiation (PAR), turbidity, and total suspended solids (TSS) were collected by NOAA GLERL and CIGLR. These data, plus dissolved and particulate microcystin concentrations, are published by NOAA GLERL and publicly available at https://www.ncei.noaa.gov/access/metadata/landing-page/bin/iso?id=gov.noaa.nodc:GLERL-CIGLR-HAB-LakeErie-water-qual. 12 ml of water was filtered (0.22 μm Nylon syringe filters; Thermo Fisher Target 2) immediately upon collection (Reed et al., 2023) for analysis of dissolved nutrient concentrations and stored frozen until analysis. A Lachat Quikchem 8500 was used to measure concentrations of NH_4^+ (alkaline phenol and DCIC method 31-107-06-1-G), NO_2^-, NO_3^- (sulfanilamide/NED Cd reduction method 31-107-04-1-E), ortho-phosphate (ortho-P; molybdate method 31-115-01-1-I), and urea (diacetyl monoxime/thiosemicarbazide method 31-206-00-1-A). Water for nitrification rate incubations was collected with a 10-L Niskin bottle, decanted into 20-L polyethylene carboys, and transported to Wright State University for isotope amendment, incubation, and analysis.

To determine AOO community structure and *amoA* abundance in the western basin, lake water was filtered (60–360 ml) through Sterivex filters (0.2 μm, EMD Millipore). Air was flushed through filters to clear residual water, then filled with RNALater (Thermo Fisher) and capped to preserve genetic material. Filters were placed on dry ice in the field, then frozen at -80 °C until DNA extraction.

For the larger lake surveys, sampling was conducted aboard the *CCGS Limnos* in conjunction with the Environment and Climate Change Canada (ECCC) HABs program. Cruises occurred in October 2015, August/September 2017, and October 2017. Six stations (215, 885, 387, 880, 1057, and 452) were sampled in 2015, seven (215, 966, 970, 972, 880, 1057, and 452) in Aug/Sept 2017, and two (880 and 452) in Oct 2017 (Fig. 1). During each cruise, stations were selected to establish a gradient across the east-west span of Lake Erie. During Oct 2017, inclement weather limited sampling to two stations, one in the central basin (880; Fig. 1), and one in the eastern basin (452; Fig. 1). At each station, water was collected from two depths (~1 m below the water surface and ~2 m above the sediment surface) using a 10-L Niskin bottle. 10 L of water was collected from each depth and transferred into 3-L polyethylene containers. Ambient nutrient and DNA samples were immediately filtered and stored frozen until analysis, as described above. Other physicochemical parameters (water temperature, conductivity, oxygen concentration, oxygen saturation, turbidity, transmittance, chlorophyll-*a*, phycocyanin, and pH) were collected by ECCC, along with chlorophyll-*a* specific estimates of phycocyanin-Cyanobacteria, Heterokontophyta and Pyrrophyta, which includes diatoms and chrysophytes), and total algae biomass via fluoroprobe (Zastepa et al., 2023).

Incubations

Nitrification rates were quantified via the addition of $^{15}NH_4^+$. A control bottle containing site water, but no isotope amendment, was used to ensure no ^{15}N contamination of experiments. For nitrification rates, site water was decanted into triplicate, colorless, translucent, 125 ml Nalgene bottles and amended with trace amounts of $^{15}NH_4Cl$ (98 atom%), which equated to approximately 20% of the ambient NH_4^+ pool, except in August and September, when NH_4^+ pools were often depleted (SI Table 1). Samples from each bottle were filtered immediately (0.22 μm) and frozen. Bottles were incubated for 16–25 hours (SI Table 1) in simulated lake conditions (outdoor water bath) before being sampled again. Samples were filtered (0.22 μm) into polystyrene tubes for total NH_4^+ concentration (i.e., $^{14}N + ^{15}N$) and immediately frozen. Additional 30 mL samples for $^{15}NO_x$ accumulation from tracer additions were filtered into 50 ml centrifuge tubes and frozen until pre-analysis preparation (see below).

Initially, the amount of added $^{15}NH_4^+$ that accumulated as $^{15}NO_2^-$ and $^{15}NO_3^-$ was determined separately (as described below). Based on results from 2015 and 2016, samples from 2017 were analyzed for total $^{15}N\text{-}NO_x$ ($NO_2^- + NO_3^-$) accumulation, rather than for $^{15}NO_2^-$ and $^{15}NO_3^-$ separately.

Sample preparation and nitrification rate calculations

Nitrification rates were measured as the accumulation of $^{15}NO_2^-$ and $^{15}NO_3^-$ from added $^{15}NH_4^+$ tracer. To quantify $^{15}NO_2^-$ accumulation, a sodium azide (NaN_3) solution was used to convert all NO_2^- in each sample to N_2O (McIlvin and Altabet, 2005). For $^{15}NO_3^-$ accumulation, a cadmium (Cd) reduction step, coupled to the azide method, was used to first reduce all NO_3^- to NO_2^- before converting NO_2^- to N_2O (Granger and Sigman, 2009; Heiss and Fulweiler, 2016). Post-transformation, samples were sent to the University of California - Davis Stable Isotope Facility for analysis of ^{15}N-labeled (masses 45, 46) and unlabeled (mass 44) N_2O. Control (no amendment) incubations were included at all steps to ensure lack of ^{15}N contamination. Nitrification rates were calculated according to Heiss et al. 2022.

Rates were corrected for reduction efficiency of the NaN_3 reaction and are reported in units of nM day^{-1}.

In 2015 and 2016, $^{15}NH_4^+$ converted to and accumulated as NO_2^- and NO_3^- was quantified separately. Accumulation rates of $^{15}NO_2^-$ were frequently, but not always, detectable and were generally ~5% of $^{15}NO_3^-$ accumulation rates. Therefore, in 2017, only total $^{15}NO_x$ accumulation was measured, and for 2015 and 2016, nitrification rates are presented as the sum of ^{15}N accumulation in both NO_2^- and NO_3^- pools.

Molecular analysis

DNA was extracted from Sterivex filters with the Qiagen Puregene© Core A kit and a modified version of the manufacturer's protocol (based on Ward et al. 2000). Residual RNA Later was removed from the filters with a phosphate buffer solution rinse, followed by the addition of cell lysis buffer. Proteinase K was then added, and filters were incubated for consecutive 1 h cycles at 55 and 65 °C.

Following extraction, DNA yields were quantified via spectrophotometry (Thermo Fisher Nanodrop 2000) and used to determine the abundance of functional genes for ammonia oxidation (*amoA)* in both bacterial and archaeal lineages via qPCR. Cleaned and cloned PCR amplicons were used to create plasmid standards for qPCR. For archaeal *amoA*, a 635 base-pair (bp) region was amplified with Arch-amoAF and Arch-amoAR primers (Francis et al., 2005, SI Table 2). A 491 bp region was amplified with amo-AF and amo-A2R primers (Rotthauwe et al., 1997, SI Table 2) for determination of bacterial *amoA*.

qPCR analyses were performed on 96-well plates. Serial dilutions of standards were plated alongside samples and negative (non-template containing) controls. Negative controls, five standards, and samples were plated in triplicate. The reaction mixture was formulated with Luna Universal qPCR Master Mix (New England Biolabs) following manufacturer instructions. 5–25 ng of template was added, and each reaction was performed on an Eppendorf realplex^2 thermocycler. Archaeal and bacterial *amoA* qPCR programs were carried out as follows:

AOA *amoA*: 40 cycles of 95 °C for 2 min, 95 °C for 30 s, 53 °C for 45 s, 72 °C for 1 min; 72 °C for 5 min; melting curve (Francis et al., 2005).

AOB *amoA*: 40 cycles of 95 °C for 2 min, 94 °C for 45 s, 56 °C for 30 s, 72 °C for 1 min; 72 ˚C for 5 min; melting curve (Beman et al., 2008).

Gene copy number was determined as:

Copy number = (ng * number mol^{-1})/(bp * ng g^{-1} * g mol^{-1} of bp)

and is given in units of gene copies per ml of sample water.

Statistical analysis

All statistical analyses were performed in R version 4.2.2 (R Core Team, 2022). Duplicate and triplicate nitrification samples were heterogeneous within each station and sampling event and were thus treated as individual data points. Western basin data collected during NOAA GLERL and CIGLR weekly

cruises were analyzed separately from data collected during ECCC cruises due to different temporal sampling patterns and accompanying metadata for comparative analysis.

For western basin samples, nitrification rates failed assumptions of normality, even after log-transformation and normalization. Accordingly, negative binomial general linear models ("mass" package; Ripley et al., 2013) were used to determine variability in spatial and temporal gradients for rates. The effect of month as a random effect on nitrification rates from each station was explored via mixed models; month was only responsible for 3% of variance in rates by station, so temporal conditions (month and year) were analyzed as fixed effects on measured nitrification rates. For ECCC cruise samples, due to small sample size (n = 2 or 3 for each station/depth at each time point), and based on the hypothesis of basin-driven patterns, a nonparametric Kruskal-Wallis test was used to determine spatial differences in rates, which were grouped by depth or basin instead of station.

For *amoA* gene abundance, standard linear models (lm function in base R "stats" package) were employed following log transformation. Relationships between nitrification rates, *amoA* gene copies, and environmental variables were explored with Spearman's rank correlations ("Hmisc" package; Harrel Jr., 2019). Tukey's HSD post-hoc tests for each model were performed using the "emmeans" package (Lenth et al, 2019).

RESULTS

Ambient conditions during western Lake Erie sampling

Environmental parameters for sampling stations and dates for nitrification experiments occurred simultaneously with NOAA GLERL monitoring and are also reported in Hoffman et al. (2022). Data tables for ambient water quality parameters used in statistical analyses are included in SI Tables 3 and 4.

Water column dissolved inorganic N (DIN), urea, and ortho-P concentrations in the western basin generally followed expected patterns, with concentrations decreasing with distance from the Maumee River. Phycocyanin (a diagnostic pigment for cyanobacteria), particulate and dissolved microcystins, and chlorophyll *a* followed similar patterns. Greatest phytoplankton biomass concentrations were measured at the westernmost station (WE6) at the height of the bloom, corresponding with depleted or undetectable ambient NH_4^+ concentrations.

Ambient conditions during ECCC cruise sampling

In October 2015, six stations ranging in depth from 5.5 m (387) to 52 m (452) were sampled, and water quality data are reported in supplemental tables. Nutrient concentrations were greatest at station 215 nearest the Maumee River inflow to western Lake Erie and decreased with distance, except for NH_4^+ and NO_3^-, which had concentration spikes in bottom waters at stations 1057 and 452 (SI Table 5). Phytoplankton biomass was concentrated in the western basin and decreased moving eastward, with cyanobacteria and diatoms comprising most of the algal biomass at most stations and depths (SI Table 6).

During the August 2017 cruise, seven stations with a depth range of 8 m at the shallowest station in the western basin (215) to 52 m in the eastern basin (452) were sampled. O_2 concentrations in surface waters were near or above 100% saturation, and deep waters from stations ≤ 11 m deep remained oxygenated. However, at the two central basin stations (880 and 1057), O_2 concentrations decreased to hypoxic (and near anoxic) levels in bottom water (SI Table 7). As in the previous cruise, cyanobacteria and diatoms dominated the phytoplankton community at most sampling sites (SI Table 8). Nutrient concentrations were lower in the westernmost part of the western basin. East of station 215, NO_3^- concentrations in the western basin were 13–15 μM compared to 6–8 μM in the central basin, regardless of depth. In bottom waters at station 452 (52 m), there was a deep pool of NO_3^-, with higher concentrations than any others measured that week (SI Table 7).

In October 2017, due to inclement weather, only one central basin (880) and one eastern basin (452) station were sampled. NH_4^+ concentrations were 3x greater at station 880 than at 452, but NO_3^- concentrations at station 452 were 2–7x greater than at 880, with the largest pool of NO_3^- observed at depth, as also observed in August (SI Table 7).

Nitrification rates in western Lake Erie

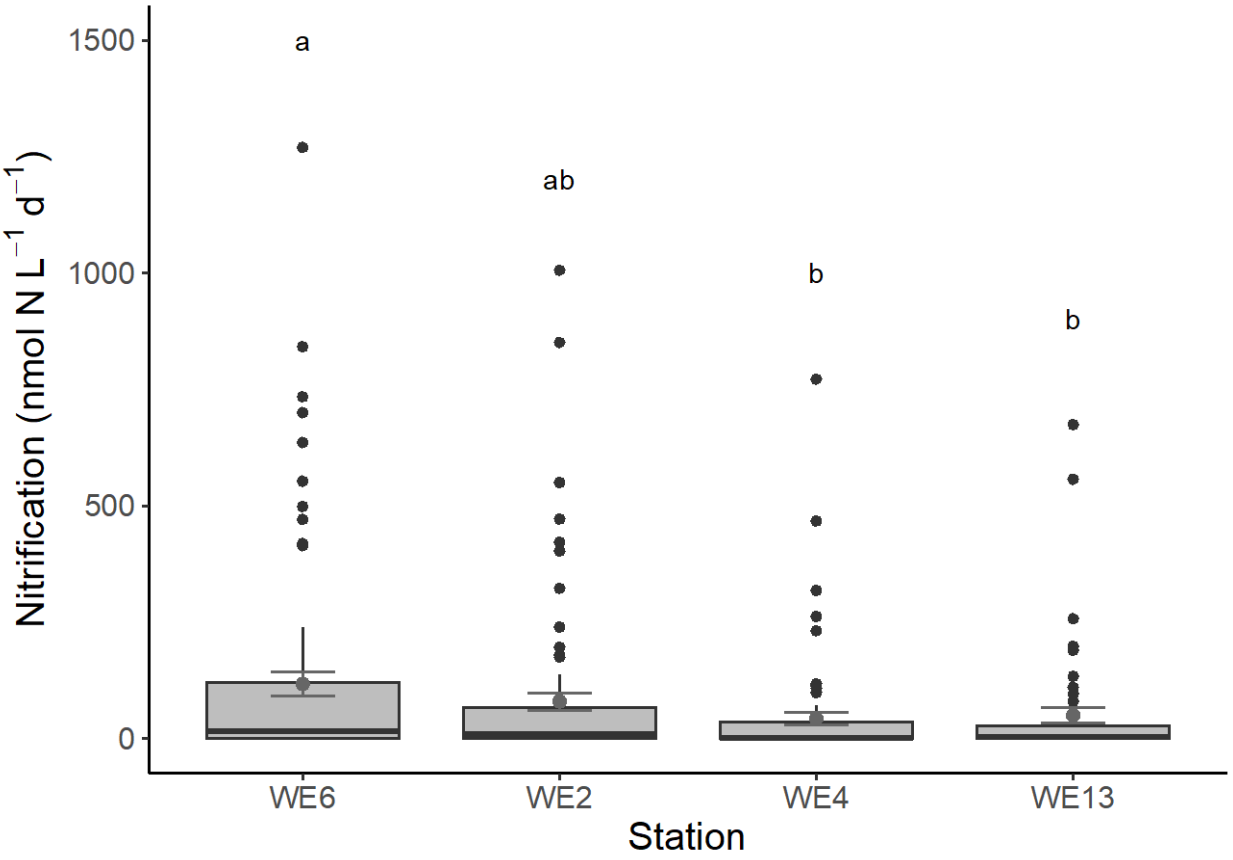

Figure 2. Nitrification rates (nmol L^{-1} d^{-1}) at four western Lake Erie sampling stations. Means (± SE) are indicated on each boxplot. Letters reflect differences in nitrification rates between stations (Tukey's HSD post-hoc tests). *n* for each station is as follows: WE6 = 90, WE2 = 96, WE4 = 90, WE13 = 60.

Nitrification rates were not influenced by depth across all stations and months, but rates from samples collected ~ 1 m above the sediment were greater ($p = 0.006$) than surface measurements in 2015. Nitrification rates at WE6 were greater than those at WE4 and WE13 ($p = 0.0025$ and 0.030, respectively), but stations WE2, WE4, and WE13 were not different from each other ($p > 0.20$; Fig. 2). Nitrification peaked in late spring/early summer, decreased to low or undetectable levels during peak cyanoHABs (August and September), and then increased in October once the bloom dissipated (Fig. 3). When all three sampling years were considered together, nitrification rates in June and July were greater than those in August and September ($p \leq 0.03$ for all pairings). Within each year, nitrification was greater in July than in September in 2015 ($p < 0.001$, Fig. 3), while June and July had greater rates than August in 2016 ($p < 0.001$ and $p = 0.048$, respectively; Fig. 3). In 2017, there were no differences in nitrification rates between sampling months (SI Fig. 1). Differences in nitrification rates at individual stations between years were largely driven by rates at WE4 but were not statistically robust; however, these relationships may be ecologically relevant ($p = 0.053$ – $p = 0.058$) for the following: at WE4, nitrification rates in June 2016 were greater than those in June 2015 and June 2017; July 2017 nitrification rates were greater than those in July 2015 or July 2016; and nitrification rates in August 2017 were greater than those in August 2015 (Fig. 3 and SI Fig. 1).

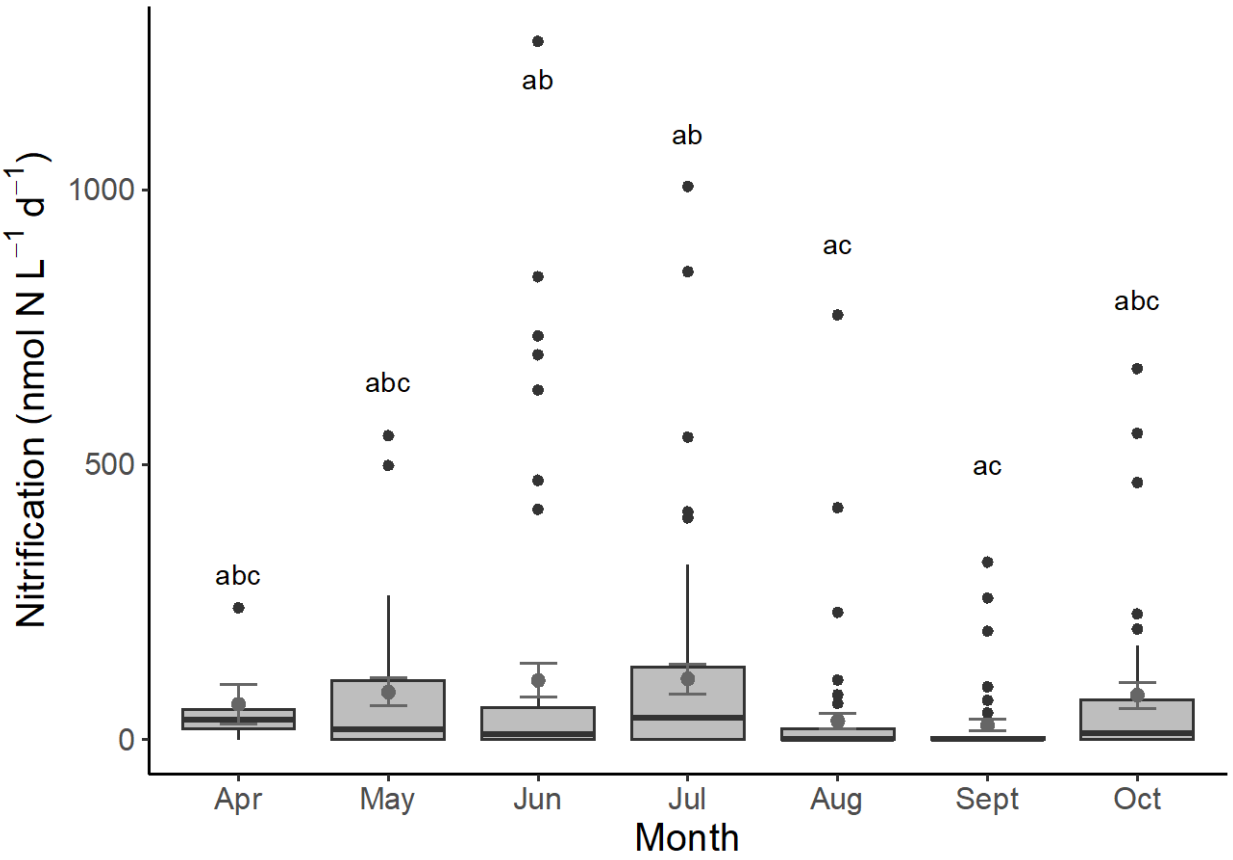

Figure 3. Nitrification rates in each month at each station across all three years. Means (± SE) are indicated on each boxplot. Letters reflect differences in nitrification rates between months (Tukey's HSD post-hoc tests). *n* for each month is as follows: April = 6, May = 36, June = 66, July = 60, August = 66, September = 54, October = 48.

In 2015, nitrification rates ranged from undetectable to 851 nmol L^{-1} d^{-1} (48.5 ± 15.0, mean ± SE; $n = 72$), with the greatest rates measured at WE2 in July (Figs. 2 and 3 and SI Fig. 1). Nitrification rates in August and September were much lower and often undetectable, although rates as high as 230 nmol L^{-1} d^{-1} were observed at WE4. In 2016, rate maxima (1270 nmol L^{-1} d^{-1} at WE6 in June) were nearly double those in 2015 (mean 84.8 ± 18.0; $n = 119$). During July and August, nitrification rates remained below 35 nmol L^{-1} d^{-1} but increased to 200–300 nmol L^{-1} d^{-1} in September and 675 nmol L^{-1} d^{-1} at WE13 in October. Nitrification rates up to 1,000 nmol L^{1} d^{-1} were measured in 2017 (79.7 ± 16.1; $n = 106$); as in 2015, this rate maximum was observed at WE2 in July. Compared to previous years, some of the greatest rates (up to 772 nmol L^{-1} d^{-1}; SI Fig. 1) were observed at stations furthest from the Maumee River (WE4 and WE13) in August and September 2017, while rates at the westernmost stations increased again in October. Nitrification rates were positively correlated with ambient NH_4^+ ($p = 0.007$), NO_2^- ($p = 0.0002$), NO_3^- ($p = 0.0051$), and urea ($p = 0.023$) concentrations, as well as conductivity ($p = 0.022$), and were negatively correlated with phycocyanin ($p = 0.025$, Fig 4).

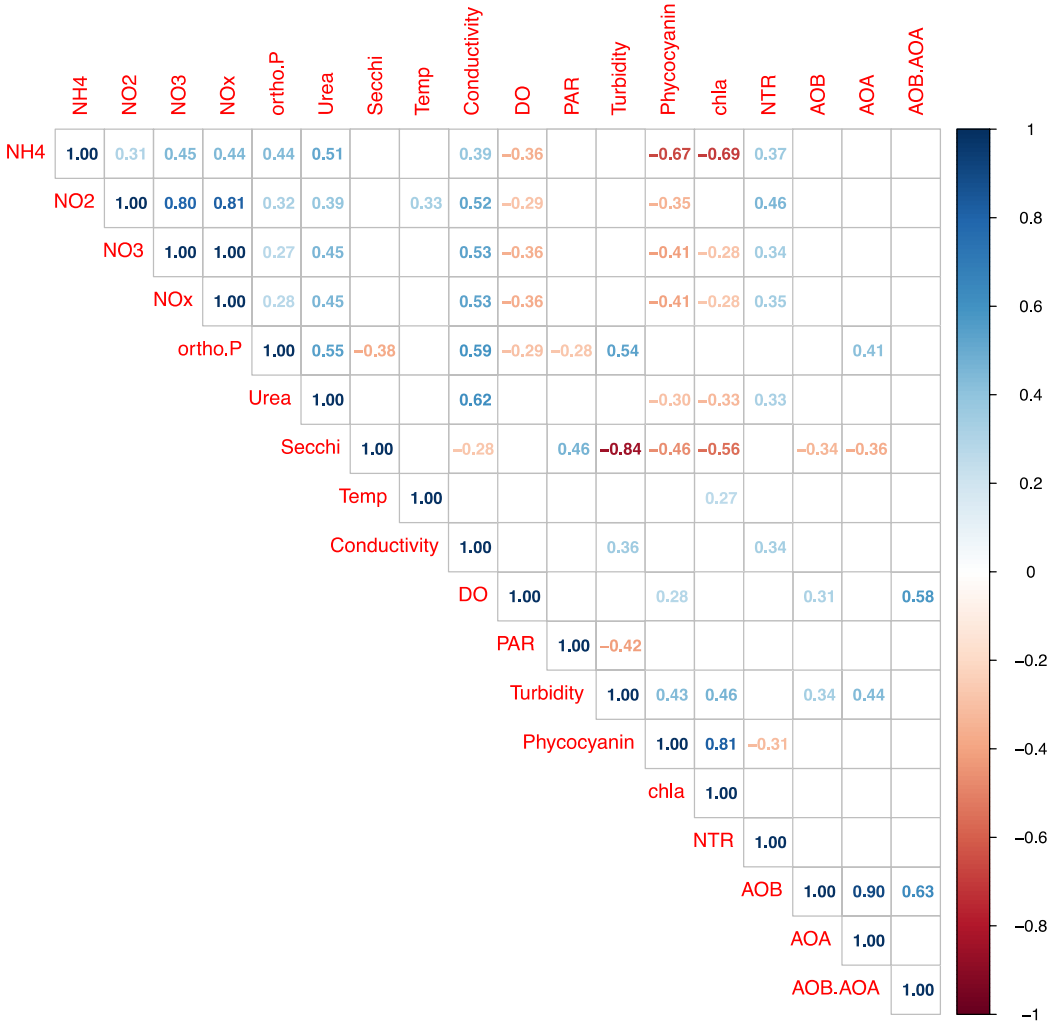

Figure 4. Spearman's rank correlations for environmental variables, nitrification rates, and gene counts in WLE. Abbreviations are as follows: ammonium (NH4), nitrite (NO2), nitrate (NO3), nitrate + nitrite (NOx), water temperature (Temp), dissolved oxygen (DO), photosynthetically active radiation (PAR), chlorophyll-*a* (chla), nitrification rate (NTR), copies of *amoA* in ammonia-oxidizing bacteria and archaea (AOB and AOA, respectively), and the ratio of AOB to AOA (AOB.AOA). Values shown for each pairing are the correlation coefficient (rho) at $p < 0.05$.

Nitrification rates across Lake Erie on ECCC Cruises

During cruise events, nitrification rates ranged from undetectable to 878 nmol L^{-1} d^{-1}, with the greatest rates measured in August 2017 in the western basin. In October 2015, there was no effect of depth on nitrification rates, but rates tended to be greater in deep water samples at stations 387, 885, and 880 (SI Fig. 2). Nitrification rates at depth were higher overall in August 2017 ($p = 0.027$), and at the deepest station (452; ~52 m). Nitrification rates in bottom water samples were 100 times greater than in

surface water. In October 2017, nitrification rates were greater ($p = 0.003$) at the eastern basin station (452) than the central basin station (880). When all cruise data is considered, nitrification rates were positively correlated with reaction products (NO_2^- and NO_3^-), as well as ortho-P, but not with any other physicochemical or biological parameter (Fig. 5).

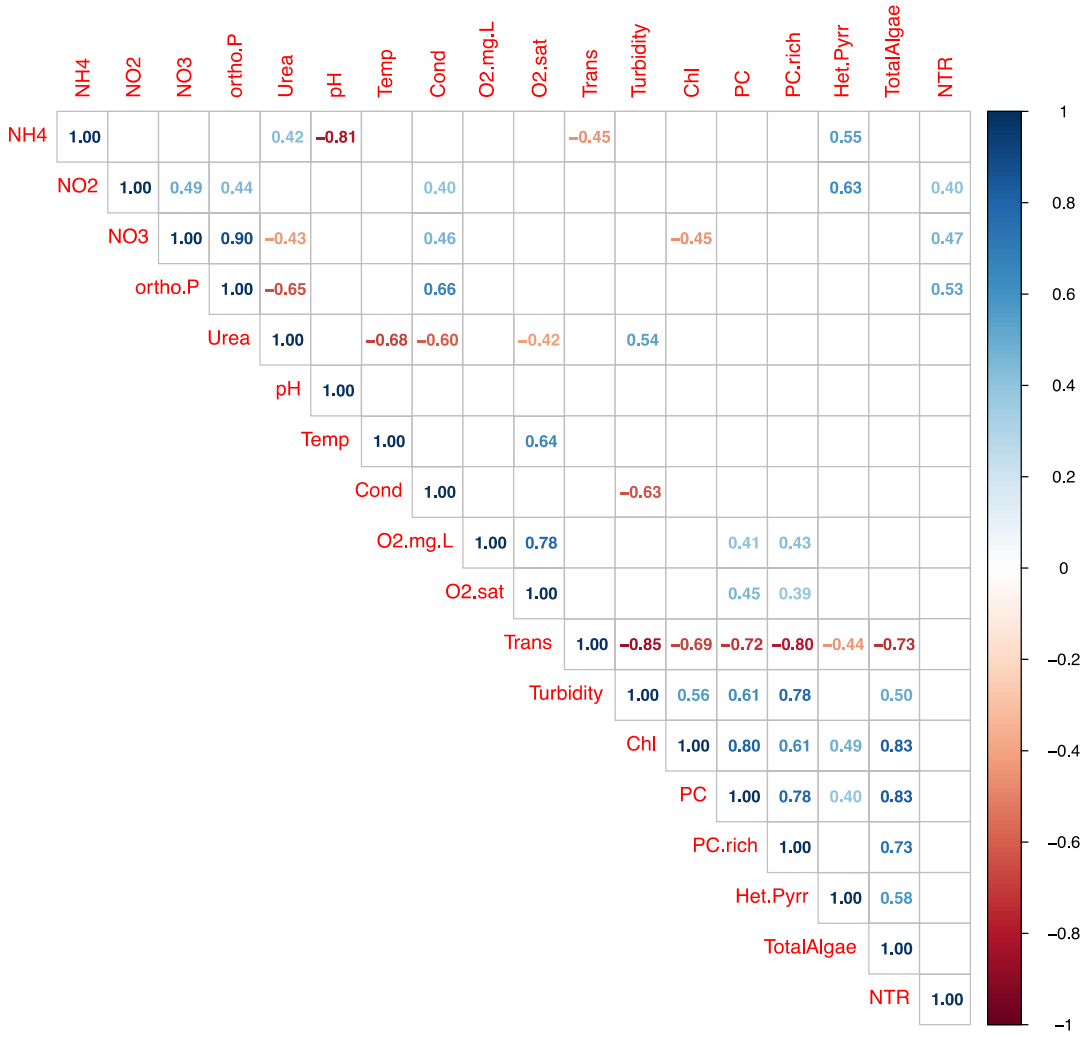

Figure 5. Correlation plot of nitrification rates and environmental variables in October 2015, August 2017, and October 2017 from ECCC cruises. Abbreviations/subgroups are as follows: water temperature (Temp), conductivity (Cond), oxygen concentration (O2.mg.L), oxygen saturation (O2.sat), transmittance (Trans), chlorophyll-*a* (chla), phycocyanin (PC), phycocyanin-Cyanobacteria (PC.rich), Het.Pyr (Heterokontophyta and Pyrrophyta which includes diatoms, chrysophytes, and dinoflagellates; nomenclature from Zastepa et al. 2023b), ammonium (NH4), nitrite (NO2), nitrate (NO3), and nitrification rate (NTR). Values shown are coefficients (rho) from Spearman's correlations at $p < 0.05$.

Ammonia oxidizer abundances in western Lake Erie

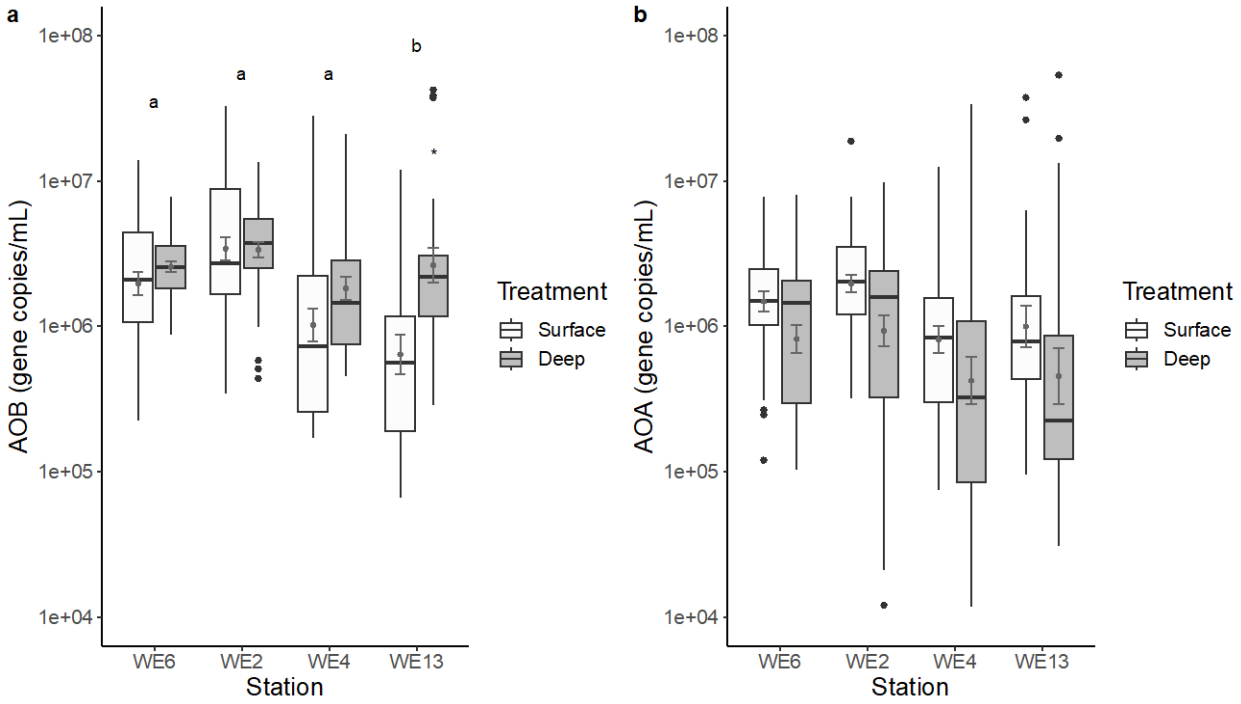

Figure 6. (a) AOB and (b) AOA *amoA* copies at each station across all three sampling years. Means (± SE) are indicated on each boxplot. Letters reflect differences in amoA copies between stations (Tukey's HSD post-hoc tests). *n* for each amoA group at each station is as follows: WE6 = 72, WE2 = 84, WE4 = 72, WE13 = 47.

For bacterial *amoA*, spatial and depth gradients influenced gene counts in the western basin. Across all three years, and with increasing distance from the Maumee River, bacterial *amoA* gene counts at WE6 and WE2 were not different from each other, nor were WE4 and WE13, but each of the former grouping had greater AOB *amoA* copies than the latter ($p < 0.03$, Fig. 6a). The two deepest stations (WE4 and WE13) had greater AOB *amoA* gene copy numbers in near-bottom versus surface samples ($p < 0.05$, Fig. 6a). Archaeal *amoA* gene copies were not different between stations, but within each station, there were more AOA *amoA* gene copies in surface versus near-bottom samples (Fig. 6b).

AOB gene copies were greater in 2016 than the other two sampling years, and there was no difference between 2015 and 2017 (SI Fig. 3). AOA *amoA* abundances were also greatest in 2016, but all three sampling years were different from each other, with 2017 having lower abundances than the other two (SI Fig. 3). In 2016 and 2017, AOB (Fig. 6a) and AOA (Fig. 6b) *amoA* gene copies in bloom months (July–September) were not different from each other ($p > 0.10$), nor were they different from those in mid-spring (May). However, *amoA* abundances in June were lower than in other months ($p < 0.003$ for all pairings). AOB *amoA* abundances were not correlated with nitrification rates but were positively related to AOA gene copies ($p < 0.0001$), dissolved oxygen concentrations ($p = 0.038$), and turbidity ($p = 0.023$), and negatively correlated with Secchi depth ($p = 0.024$; Fig. 4). AOA gene counts were similarly not related to nitrification rates, were positively correlated with turbidity ($p = 0.0026$) and ortho-P concentrations ($p = 0.004$), and negatively related to Secchi depth ($p = 0.014$; Fig. 4).

AOB vs. AOA in western Lake Erie

Overall, AOB *amoA* gene copies ml^{-1} were greater ($p < 0.001$) than AOA in the western basin. To explore potential differences in community composition, the ratio of AOB:AOA gene copies were calculated for each sampling event. The median ratio across the entire dataset was 1.74. In 2015 (when we

only collected DNA in August and September), AOO communities were near equal in abundance, with a median ratio of 0.97. In 2016 and 2017, the median ratio increased to 1.55 and 3.78, respectively. Across all three years, there was no difference in ratios by station, but within each station, higher ratios were observed in near-bottom versus surface waters (Fig. 7), an effect driven mostly by high bottom water ratios in 2017 (Fig. 7). Seasonally, there was no difference across months, but the greatest ratios were observed in September at WE4 in 2017 (Fig. 7). This peak ratio did not coincide with greatest nitrification rates measured that year.

Ratios in 2015 were not different from those in 2016, but ratios in 2017 were greater at depth ($p < 0.001$) than those in other years. The AOB:AOA ratio ranged from 0.28 – 2.30 in 2015, 0.34 – 33 in 2016, and 0.22 – 74 in 2017. The effect of depth differed by year, with surface samples having generally greater ratios than deep samples in 2016, while samples taken at depth in 2017 had markedly greater AOB:AOA (Fig. 7, SI Fig. 4). *amoA* ratios were correlated with AOB gene copies ($p < 0.0001$) but not with AOA gene copies or any other environmental parameter (Fig. 4).

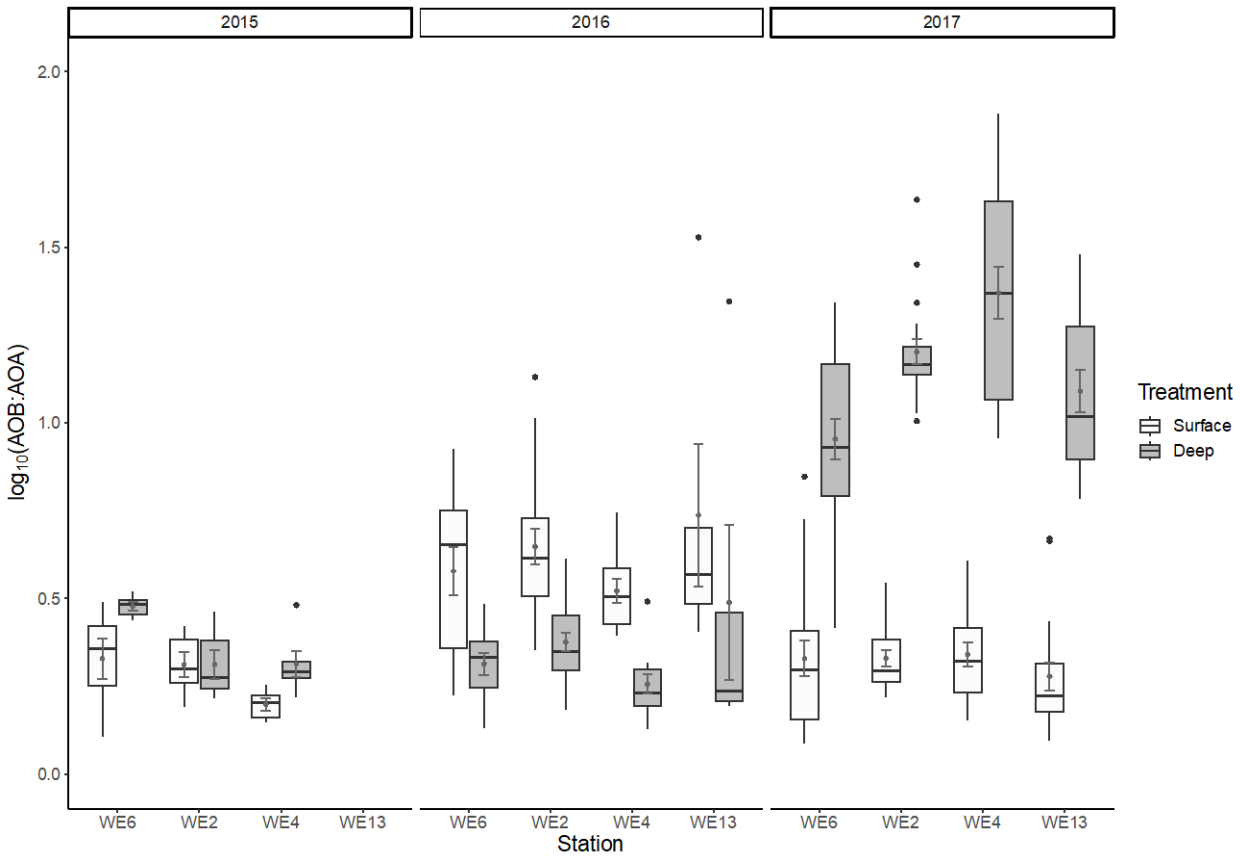

Figure 7. Ratio of AOB:AOA gene copies at each station and depth in each year. In September 2017, the ratio in near-bottom water at WE4 reached 74, but the y-axis was limited at 40 to preserve scale. *n* for each year is as follows: 2015 = 36, 2016 = 96, 2017 = 143.

DISCUSSION

During three study seasons (2015–2017), nitrification rates across Lake Erie and abundances of genes associated with nitrification (western basin only) were measured to identify spatial and temporal patterns and possible drivers of nitrification. Results from this study indicate that, despite the ubiquitous presence of AOO, nitrification in western Lake Erie is greatest when cyanoHABs are not present, suggesting that nitrification as a link to denitrification is unlikely to compensate for external and internal

(e.g., NH_4^+ regeneration in the water column; Hoffman et al., 2022) N loading with regard to mitigating cyanoHABs. These results provide new insights into the spatial dynamics surrounding NH_4^+ cycling and trophic status across all three basins of Lake Erie.

Nitrification dynamics in western Lake Erie

Nitrification rates were expected to follow seasonal trends, peaking in pre- and post-bloom periods, and decreasing when cyanoHABs were present (as in Hampel et al., 2018). During summer, when cyanoHAB biomass was greatest (August and September), nitrification rates were the lowest. Ambient water column NH_4^+ concentrations were depleted during cyanoHABs, suggesting substrate limitation of nitrification. Although nitrification was not correlated with chlorophyll *a*, nitrification rates were negatively correlated with phycocyanin (cyanobacteria pigment), which peaked during August and September. During the pre-bloom season, greatest nitrification rates were measured in the westernmost part of the basin, nearest to the primary external nutrient source (Maumee River). However, when blooms were present, greatest nitrification rates were observed at stations furthest from the river inflow.

As expected, positive relationships were observed between nitrification rates and substrate (NH_4^+) and end product (NO_2^- and NO_3^-) concentrations. Relationships between nitrification rates and NOx concentrations are commonly reported (e.g., Pauer and Auer, 2000; Newell et al., 2011; Hampel et al., 2018; Cavaliere and Baulch, 2019) and illustrates the importance of nitrification as a source of substrate for denitrification. Molecular oxygen is obligate for ammonia oxidation, but no relationship was observed between nitrification rates and dissolved oxygen concentrations. The western basin is shallow and generally well-mixed to the sediment surface, and dissolved oxygen is uniform throughout the water column. There was also no relationship between nitrification rates and temperature, which may be due to large cyanoHABs in the warmest months and is consistent with observations from another eutrophic lake afflicted with *Microcystis*-dominated blooms (Taihu; Hampel et al., 2018).

Relationships between nitrification rates and pH were also explored, since the optimal range for nitrification generally falls between pH 7.5 and 9, depending on AOO community structure (Shammas et al., 1986; Antoniou et al. 1990; Park et al. 2008). pH data for the water column was not collected as part of the GLERL sampling, so real-time buoy data from WE2, WE4, and WE13 were accessed. No discernable patterns, or much variation in pH levels, were observed, with values ranging from 7.7 to 9.1 but mostly remaining between 8 and 9 across sampling seasons and years (CIGLR and NOAA GLERL, 2019b). The stability of pH within the optimum range for nitrification indicates that pH is likely not a main driver of observed seasonal differences in nitrification rates.

Compared to other lakes in which $^{15}NH_4^+$ tracer addition methods were employed, late spring/early summer nitrification rates in western Lake Erie greatly exceeded those measured in oligotrophic Lake Superior (USA, 0 – 51 nmol L^{-1} d^{-1}; Small et al., 2013) but were similar to those in saline Mono Lake (USA, 0 – 480 nmol L^{-1} d^{-1}; Carini and Joye, 2008) and Lake Croche (Canada, 0 – 333 nmol L^{-1} d^{-1}; Massé et al., 2019). Nitrification rates in western Lake Erie were similar to the range of rates from mesotrophic Lake Lacawac (1 – 568 nmol L^{-1} d^{-1}; Heiss et al., 2022) and other eutrophic lakes, including lakes Okeechobee (30 – 120 nmol L^{-1} d^{-1}; James et al. 2011) and Taihu (China, 0 – 3,750 nmol L^{-1} d^{-1}; Hampel et al. 2018). Rate maxima from western Lake Erie were about a third of the highest values reported in Taihu (Hampel et al., 2018). Higher rates at depth were also observed in mesotrophic Lake Lacawac (Heiss et al., 2022) and are commonly observed in the ocean (Ward et al., 2008) due to inhibition of nitrification at high light intensities found in surface waters (Guerrero and Jones, 1996; Merbt et al., 2012). One exception to these patterns is Lake Onondaga, where sediment nitrification was observed, but apparently with no corresponding activity in the water column. The authors attribute this lack of water column nitrification to low nitrifier densities, which contrasts with the present and many other studies (Pauer and Auer, 2000).

Western basin nitrification vs. community NH_4^+ demand and water column NH_4^+ regeneration

In Hoffman et al. 2022, community potential NH_4^+ uptake rates were reported for the water column at the same western basin stations and time points as nitrification rates measured here. Nitrification rates were compared to potential NH_4^+ uptake to determine the proportion of this community NH_4^+ uptake attributable to nitrification. As expected, the percentage of NH_4^+ uptake explained by nitrification was greatest in late spring and early summer, but declined to, on average, less than 5% of total NH_4^+ demand during peak bloom months (Fig. 8). In 2015, the most intense cyanoHAB year, the percentage of NH_4^+ demand accounted for by nitrification ranged from 0 to 7.04% (0.413 ± 0.133%, mean ± SE; n = 71). In 2016 and 2017, the maximum contribution of nitrification increased to 55.2% (3.61 ± 0.745; n = 119) and 59.6% (3.81 ± 1.10; n = 143), respectively (Fig. 8), early in the season (WE2 in June 2016) and at stations furthest from the Maumee River mouth (WE13 in August 2017). The contribution of nitrification to community potential NH_4^+ uptake rates in western Lake Erie spans a much greater range than that reported in Lake Taihu, where values from 0.2 – 15% were observed (Hampel et al., 2018).

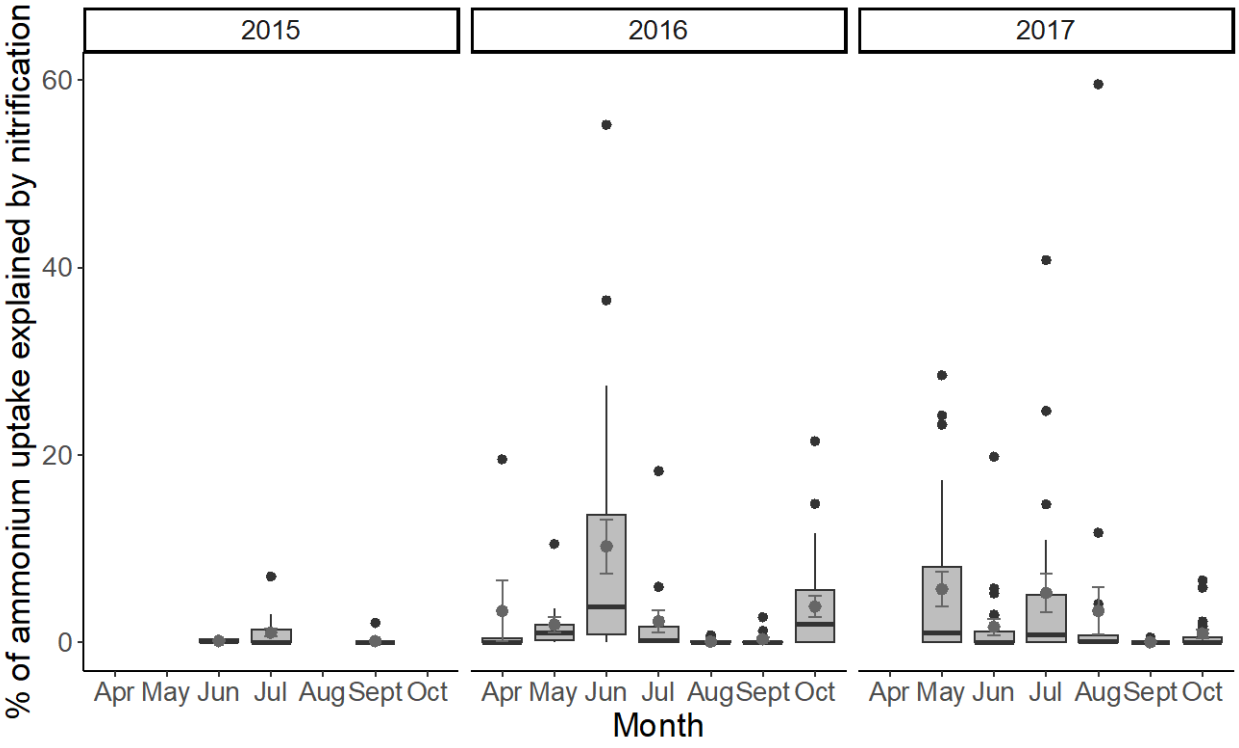

Figure 8. The percentage of community potential NH_4^+ uptake explained by nitrification in each month within each sample year. n for each month in each year is as follows: 2015 (June = 18, July = 18, August = 18, September = 18); 2016 (April = 6, May = 12, June = 24, July = 18, August = 24, September = 12, October = 24); 2017 (May = 24, June = 24, July = 24, August = 24, September = 24, October = 24).

Nitrification rates during ECCC cruises

Nitrification rates did not vary by basin ($p > 0.15$), despite highest nutrient inputs in the western basin, perhaps because western basin nitrification rates were inhibited by summer cyanoHABs. Nitrification rates measured from these experiments (118 ± 31.0 nmol L^{-1} d^{-1}) are within the ranges reported in the water columns of other eutrophic lakes, although rate maxima (up to 878 nmol L^{-1} d^{-1}) were much lower than those from Lake Taihu (3,750 nmol L^{-1} d^{-1}; Hampel et al., 2018), Lake Okeechobee (1,280 nmol L^{-1} d^{-1}; Hampel et al., 2020), and Lake Mendota (1,700 – 5,000 nmol L^{-1} d^{-1}; Hall, 1986). Nitrification rates in Lake Erie also were similar to those in mesotrophic Lake Lacawac (1 – 568 nmol L^{-1}

488 d^{-1}; Heiss et al., 2022) and saline Lake Mono (60 – 335 nmol L^{-1} d^{-1}; Carini and Joye, 2008). However,
489 nitrification rates in Lake Erie, particularly those from the eastern basin, were much greater than those in
490 oligotrophic Lake Superior (0 – 51 nmol L^{-1} d^{-1}; Small et al., 2013).
491
492 **Ammonia-oxidizer community abundance and competition dynamics in western Lake Erie**
493 We hypothesized that AOB would outnumber AOA due to differences in relative affinity for
494 NH_4^+ and the AOB community's competitive advantage in high-NH_4^+ environments. Ambient NH_4^+
495 concentrations in western Lake Erie ranged from undetectable to 7.30 µM, within the established K_m for
496 AOB but thought to be greater than that of AOA (AOA isolates: 0.05–0.14 µM; Martens-Habbena et al.,
497 2009). However, some AOA isolates have higher K_m values, which may explain some of the variability in
498 AOB:AOA (Jung et al. 2022). Higher abundances of AOO were expected during non-bloom periods, but
499 AOO gene copies were lowest in June, when some of the highest nitrification rates were measured. Both
500 AOB and AOA were positively correlated with turbidity, which may be related to incoming nutrient and
501 sediment loads from the Maumee River and/or sediment resuspension.
502 Comammox *amoA* gene abundances were not quantified in this study, but nitrification rates were
503 high at times in this study. All nitrifiers may play an important role in aquatic systems, and comammox
504 should be investigated further in future lake studies. Comammox is important in wastewater treatment
505 plants (Yang et al. 2020, Su et al. 2021) and lake sediments (Lu et al. 2020, Xu et al. 2020), but the few
506 comammox studies in lake water columns suggest that abundances are low (e.g., Harringer and Alfreider
507 2021).
508 Despite the presence of AOO at all sampling stations and times, nitrification rates were low
509 during summer months and constituted a small fraction of community potential NH_4^+ uptake. There was
510 no correlation between measured nitrification rates and either bacterial or archaeal *amoA* gene copy
511 numbers. With a subset of the data (undetectable rates excluded), nitrification rates and AOA gene copies
512 were correlated ($\boldsymbol{\rho} = 0.19$). A similar study in Lake Taihu found that nitrification rates were correlated
513 with AOB but not AOA (Hampel et al., 2018), while in Lake Okeechobee, nitrification rates were
514 strongly related to AOA abundance (Hampel et al., 2020). *amoA* abundance was quantified using DNA,
515 as opposed to gene transcription via RNA, which may explain discrepancies between biogeochemical and
516 molecular results. These discrepancies also support the hypothesis that, although present and presumably
517 active, the AOO community were not effective competitors for available NH_4^+, especially during
518 cyanoHABs.
519 High abundances of *amoA* in western Lake Erie are not without precedent, as a previous study
520 found large numbers of AOB and AOA in Lake Erie sediments (Bollmann et al., 2014). Since western
521 Lake Erie is well-mixed and often turbid, particle-attached AOO communities may be introduced into the
522 water column via sediment loading from the river and/or sediment resuspension. Within the water
523 column, *Proteobacteria* (which includes AOB) can account for nearly 20% of the metagenome during
524 cyanoHABs in Lake Erie (and ~70% in hypereutrophic Lake Taihu; Steffen et al., 2012), and these
525 estimates do not account for co-occurring archaea. However, high gene abundances observed in our Lake
526 Erie study must also be considered relative to literature on copies of *amoA* per cell. *Betaproteobacterial*
527 AOB, particularly within the genus *Nitrosospira*, can have up to three copies of the *amoA* gene compared
528 to one in AOA (Norton et al., 2008; Blainey et al., 2011; Lagostina et al., 2015). Accordingly, *amoA*
529 abundances in Lake Erie do not equate to cell number. Specific community members were not identified
530 in this study, and attempts to correct AOB:AOA ratios with variations in copy number within each
531 genome do not always explain high AOB:AOA ratios (Lagostina et al., 2015). Thus, gene copy numbers
532 were not corrected based on potential genomic differences among AOB and AOA.
533 The only other known literature on water column AOO community abundances in Lake Erie
534 comes from a central basin location, where AOB outnumbered AOA (Mukherjee et al., 2015). However,
535 the authors were unable to detect any AOO in surface waters, which contrasts with the high surface water
536 abundances reported here. These discrepancies between studies may be partly attributable to different
537 methodologies for enumeration (CARD-FISH versus qPCR, where qPCR is more likely to detect inactive
538 cells and represents more than one gene copy per cell) or spatio-temporal variation in communities

(Murkherjee et al. sampled only in the central basin in July 2011 vs. full-season sampling in this study in the western basin only).

Approximate parity between AOB and AOA abundances in the western Lake Erie water column aligns with findings from work conducted in Lake Erie sediments but contrasts with results from other eutrophic lakes. At a station near WE6, AOB and AOA numbered from $10^6 – 10^7$ copies per g sediment, and the two community abundances were not different from each other (Bollmann et al., 2014). In Lake Taihu, AOA outnumbered AOB in the water column, with AOA and AOB copies ml^{-1} reaching as high as 10^7 and 10^5, respectively (Hampel et al., 2018). In a Taihu mesocosm experiment, however, AOB outnumbered AOA by up to two orders of magnitude (Chen et al., 2016). AOB gene copies in western Lake Erie were often much greater than those in Taihu by an order of magnitude, but AOA gene copies were similar between the two lakes. Similarly, AOA abundances in Lake Okeechobee exceeded those of AOB (AOA up to 10^6, AOB up to 10^5; Hampel et al., 2020), with maximum abundances in western Lake Erie greater for both AOA and AOB by an order of magnitude or more. In general, maximum AOB and AOA abundances were within the ranges of those from other lakes, including eutrophic Lake Dianchi (China, maximum 10^5 for both AOA and AOB *amoA* abundances; Yang et al. 2016), mesotrophic Lake Lacawac (USA, up to 10^6 copies ml^{-1} for both AOA and AOB; Heiss et al. 2022), and oligotrophic Lake Constance (Europe, 10^5 AOA copies ml^{-1}; Klotz et al. 2022).

While early studies of AOA indicated that they were important mostly in oligotrophic environments (Beman et al., 2008; Pester et al., 2012), more recent work has demonstrated that some AOA ecotypes thrive in eutrophic systems. AOA are abundant alongside AOB in wastewater treatment plant bioreactors (e.g., Park et al., 2006; Limpiyakorn et al., 2013; Zhang et al., 2015), and new ecotypes have been reported in eutrophic lakes, such as Lake Okeechobee (Hampel et al., 2020). Given evolving knowledge and high abundances of AOA in Lake Erie and other eutrophic lakes, AOA may play a larger role in these systems than previously thought (Zeng et al., 2012; Damashek et al., 2015; Hampel et al., 2018, 2020).

Despite some discrepancies in AOO community dynamics between this study and others conducted in eutrophic lakes, seasonal patterns of nitrification rates suggest that the presence of cyanoHABs suppresses nitrification in WLE. This observation matches with findings reported in lakes Taihu (Hampel et al., 2018) and Okeechobee (Hampel et al., 2019), both of which are also afflicted with *Microcystis*-dominated cyanoHABs and may be explained by the strong affinity of *Microcystis* for NH_4^+. Studies in culture and in lakes have reported a broad range of K_m values for *Microcystis*, with maximum values reaching 37 μM in culture (Nicklisch and Kohl, 1983) and 113 μM in lakes (Yang et al., 2017). In Maumee Bay, community K_m values changed along a seasonal gradient, beginning at very low K_m (0.32 μM) in early summer, increasing to 3.53 μM in August and 8.52 μM in October (Hampel et al., 2019). The authors suggested that this pattern illustrates community dominance of *Microcystis* during cyanoHAB development and peak bloom biomass, which reflects the strong competitive abilities of *Microcystis* for available NH_4^+. Based on previously discussed literature values, coupled with seasonally decreasing nitrification rates and NH_4^+ concentrations during the cyanoHAB season, it appears that nitrifiers in western Lake Erie were unable to compete effectively with cyanoHAB communities for NH_4^+.

SYNTHESIS

Despite high water column NH_4^+ demand in peak bloom months (Hoffman et al. 2022), nitrification comprised a small proportion of this demand. Even though bioavailable N concentrations were depleted during cyanoHABs, regeneration of the NH_4^+ pool is still occurring at rates exceeding nitrification. However, where NH_4^+ regeneration is greatest (at WE6, Hoffman et al. 2022), nitrification was also near-undetectable, further supporting the conclusion that nitrifiers cannot scavenge NH_4^+ as efficiently as cyanoHAB microorganisms. The lack of relationship between *amoA* gene copies and nitrification rates indicates that gene abundance is not a reliable indicator of activity in western Lake Erie, and future studies should consider other methodology, such as RNA or metatranscriptomic analysis when comparing rate measurements to genetic data. The ability of water column nitrification to act as a buffer against external N loading by supplying the substrate for denitrification is impeded by cyanoHABs in

western Lake Erie and similar systems; therefore, management of external N loads is crucial for mitigating the harmful effects of eutrophication. These findings support previous work demonstrating suppression of nitrification in oxic waters via competition for NH_4^+ during cyanoHABs and suggest that non-cyanoHAB biomass (e.g., other phytoplankton, such as diatoms and cryptophytes) in the central and eastern basins may also outcompete nitrifiers for available NH_4^+. Ecosystem models often neglect within-system transformation pathways, such as nitrification, and as such may lack important information needed to accurately make management decisions. Accordingly, results from this and other studies should be considered when creating and validating models to help inform management decisions.

Acknowledgements

This research was funded by Ohio Sea Grant. We thank the captains, crews, and technicians at NOAA GLERL, CIGLR, ECCC, and the *CCGS Limnos* for sampling opportunities and assistance aboard their vessels. We are grateful for Dr. Justyna Hampel and other Newell and McCarthy lab students and colleagues for their assistance with sample collection and processing.

REFERENCES

Antoniou, P., Hamilton, J., Koopman, B., Jain, R., Holloway, B., Lyberatos, G., & Svoronos, S. A. (1990). Effect of temperature and pH on the effective maximum specific growth rate of nitrifying bacteria. Water research, 24(1), 97-101.

Barbiero, R.P. and Tuchman, M.L., 2004. Long-term dreissenid impacts on water clarity in Lake Erie. Journal of Great Lakes Research, 30(4), 557-565.

Beman, J.M., Popp, B.N. and Francis, C.A., 2008. Molecular and biogeochemical evidence for ammonia oxidation by marine Crenarchaeota in the Gulf of California. The ISME Journal, 2(4), 429-441.

Bertani, I., Obenour, D.R., Steger, C.E., Stow, C.A., Gronewold, A.D. and Scavia, D., 2016. Probabilistically assessing the role of nutrient loading in harmful algal bloom formation in western Lake Erie. Journal of Great Lakes Research, 42(6), 1184-1192.

Blainey, P.C., Mosier, A.C., Potanina, A., Francis, C.A. and Quake, S.R., 2011. Genome of a low-salinity ammonia-oxidizing archaeon determined by single-cell and metagenomic analysis. PloS One, 6(2), p.e16626.

Blomqvist, P., Pettersson, A. and Hyenstrand, P., 1994. Ammonium-nitrogen: a key regulatory factor causing dominance of non-nitrogen-fixing cyanobacteria in aquatic systems. Archiv für Hydrobiologie, 141-164.

Bridgeman, J., Bridgeman, T.B., Bade, D.L. and Mobilian, C.N., 2014. Summer phytoplankton nutrient limitation in Maumee Bay of Lake Erie during high-flow and low-flow years. Journal of Great Lakes Research, 40(3), 524-531.

Chaffin, J.D., Mishra, S., Kane, D.D., Bade, D.L., Stanislawczyk, K., Slodysko, K.N., Jones, K.W., Parker, E.M. and Fox, E.L., 2019. Cyanobacterial blooms in the central basin of Lake Erie: Potentials for cyanotoxins and environmental drivers. Journal of Great Lakes Research, 45(2), 277-289.

Chen, X., Jiang, H., Sun, X., Zhu, Y. and Yang, L., 2016. Nitrification and denitrification by algae-attached and free-living microorganisms during a cyanobacterial bloom in Lake Taihu, a shallow Eutrophic Lake in China. Biogeochemistry, 131(1-2), 135-146.

Conroy, J.D., Edwards, W.J., Pontius, R.A., Kane, D.D., Zhang, H., Shea, J.F., Richey, J.N., and Culver, D.A. 2005. Soluble nitrogen and phosphorus excretion of exotic freshwater mussels (Dreissena spp.): potential impacts for nutrient remineralisation in western Lake Erie. Freshwater Biology 50: 1146-1162.

Cooperative Institute for Great Lakes Research, University of Michigan; NOAA Great Lakes Environmental Research Laboratory (2019). Physical, chemical, and biological water quality monitoring data to support detection of Harmful Algal Blooms (HABs) in western Lake Erie, collected by the Great Lakes Environmental Research Laboratory and the Cooperative Institute for Great Lakes Research since 2012. [indicate subset used]. NOAA National Centers for Environmental Information. Dataset. https://doi.org/10.25921/11da-3x54. Accessed 2019-07-11.

Cooperative Institute for Great Lakes Research, University of Michigan; National Oceanic and Atmospheric Administration Great Lakes Environmental Research Laboratory. 2019. Physical, chemical, and biological water quality data collected from moored buoy WE02, Lake Erie in the Great Lakes region from 2014-05-22 to 2018-10-15 (NCEI Accession 0190201). NOAA National Centers for Environmental Information. Dataset. https://accession.nodc.noaa.gov/0190201.

Daims, H., Lebedeva, E.V., Pjevac, P., Han, P., Herbold, C., Albertsen, M., Jehmlich, N., Palatinszky, M., Vierheilig, J., Bulaev, A. and Kirkegaard, R.H., 2015. Complete nitrification by *Nitrospira* bacteria. Nature, 528(7583), 504-509.

Damashek, J., Smith, J.M., Mosier, A.C. and Francis, C.A., 2015. Benthic ammonia oxidizers differ in community structure and biogeochemical potential across a riverine delta. Frontiers in Microbiology, 5, p.743.

Damashek, J. and Francis, C.A., 2018. Microbial nitrogen cycling in estuaries: from genes to ecosystem processes. Estuaries and Coasts, 41(3), 626-660.

Depew, D.C., Guildford, S.J. and Smith, R.E., 2006. Nearshore offshore comparison of chlorophyll a and phytoplankton production in the dreissenid-colonized eastern basin of Lake Erie. Canadian Journal of Fisheries and Aquatic Sciences, 63(5), 1115-1129.

Edwards, C.J., Ryder, R.A. and Marshall, T.R., 1990. Using lake trout as a surrogate of ecosystem health for oligotrophic waters of the Great Lakes. Journal of Great Lakes Research, 16(4), 591-608.

Francis, C.A., Roberts, K.J., Beman, J.M., Santoro, A.E. and Oakley, B.B., 2005. Ubiquity and diversity of ammonia-oxidizing archaea in water columns and sediments of the ocean. Proceedings of the National Academy of Sciences, 102(41), 14683-14688.

Glibert, P.M., Wilkerson, F.P., Dugdale, R.C., Raven, J.A., Dupont, C.L., Leavitt, P.R., Parker, A.E., Burkholder, J.M. and Kana, T.M., 2016. Pluses and minuses of ammonium and ntrate uptake and assimilation by phytoplankton and implications for productivity and community composition, with emphasis on nitrogen-enriched conditions. Limnology and Oceanography, 61, 165-197

Granger, J. and Sigman, D.M., 2009. Removal of nitrite with sulfamic acid for nitrate N and O isotope analysis with the denitrifier method. Rapid Communications in Mass Spectrometry: An International Journal Devoted to the Rapid Dissemination of Up-to-the-Minute Research in Mass Spectrometry, 23(23), 3753-3762.

Great Lakes Fisheries Commission. 2017. The State of Lake Erie in 2009. http://www.glfc.org/pubs/SpecialPubs/Sp17_01.pdf

Guerrero, M.A. and Jones, R.D., 1996. Photoinhibition of marine nitrifying bacteria. I. Wavelength-dependent response. Marine Ecology Progress Series, 141, 183-192.

Hall, G.H. 1986. Nitrification in lakes, in: *Nitrification*, 1st edition, edited by J. I. Prosser, IRL Press, Washington, DC, 127–156.

Harrison, J.J., McCarthy, M.J., Gardner, W.S., Zhang, L., Xu, H., Zhu, G. and Newell, S.E., 2018. Nitrification and ammonium dynamics in Taihu Lake, China: seasonal competition for ammonium between nitrifiers and cyanobacteria. Biogeosciences, 15(3).

Harrison, J.J., McCarthy, M.J., Reed, M.H. and Newell, S.E., 2019. Short term effects of Hurricane Irma and cyanobacterial blooms on ammonium cycling along a freshwater–estuarine continuum in south Florida. Frontiers in Marine Science, 6, p.640.

Harrison, J.J., McCarthy, M.J., Aalto, S.L. and Newell, S.E., 2020. Hurricane disturbance stimulated nitrification and altered ammonia oxidizer community structure in Lake Okeechobee and St. Lucie Estuary (Florida). Frontiers in Microbiology, 11, p.1541.

Harrell Jr, F.E., 2019. Package 'Hmisc'. CRAN 2019, 235-6.

Herbinger, M., Alfreider, A. Primer evaluation and development of a droplet digital PCR protocol targeting amoA genes for the quantification of Comammox in lakes. Sci Rep 11, 2982 (2021). https://doi.org/10.1038/s41598-021-82613-6

Hart, S.C., Stark, J.M., Davidson, E.A. and Firestone, M.K., 1994. Nitrogen mineralization, immobilization, and nitrification. Methods of Soil Analysis: Part 2 Microbiological and Biochemical Properties, 5, 985-1018.

Heiss, E.M. and Fulweiler, R.W., 2016. Coastal water column ammonium and nitrite oxidation are decoupled in summer. Estuarine, Coastal and Shelf Science, 178, 110-119.

Heiss, E. M., Zawacki, V. W., Williams, A. A., Reed, M. H., Maguire, T. J., & Newell, S. E. (2022). Ammonia-oxidizing archaea and ammonium concentration as drivers of nitrification in a protected freshwater lake. Freshwater Science, 41(4), 564-576.

Hoffman, D.K., McCarthy, M.J., Boedecker, A.R., Myers, J.A. and Newell, S.E., 2022. The role of internal nitrogen loading in supporting non-N-fixing harmful cyanobacterial blooms in the water column of a large eutrophic lake. Limnology and Oceanography, 67(9), 2028-2041.

James, R.T., Gardner, W.S., McCarthy, M.J. and Carini, S.A., 2011. Nitrogen dynamics in Lake Okeechobee: forms, functions, and changes. Hydrobiologia, 669(1), 199-212.

Kitzinger, K., Ngugi, D.K., Büsing, P., Littmann, S., Kuypers, M.M., Schink, B. and Pester, M., 2022. Quantification of archaea-driven freshwater nitrification from single cell to ecosystem levels. *The ISME Journal*, *16*(6), pp.1647-1656.

Kuypers, M.M.M., Marchant, H.K. and Kartal, B., 2018. The microbial nitrogen-cycling network. Nature Reviews. Microbiology, 16(5), p.263.

Lagostina, L., Goldhammer, T., Røy, H., Evans, T.W., Lever, M.A., Jørgensen, B.B., Petersen, D.G., Schramm, A. and Schreiber, L., 2015. Ammonia-oxidizing Bacteria of the *Nitrosospira* cluster 1 dominate over ammonia-oxidizing Archaea in oligotrophic surface sediments near the South Atlantic Gyre. Environmental microbiology reports, 7(3), 404-413.

Lenth, R., Singmann, H., Love, J., Buerkner, P. and Herve, M., 2019. emmeans: Estimated Marginal Means, aka Least-Squares Means (Version 1.3.4).

Limpiyakorn, T., Fürhacker, M., Haberl, R., Chodanon, T., Srithep, P. and Sonthiphand, P., 2013. amoA-encoding archaea in wastewater treatment plants: a review. Applied Microbiology and Biotechnology, 97(4), 1425-1439.

Li, S., Sun, Y., Lu, B., Zheng, D., & Xu, S. (2020). Change of abundance and correlation of Nitrospira inopinata-like comammox and populations in nitrogen cycle during different seasons. Chemosphere, 241, 125098.

Martens-Habbena, W., Berube, P.M., Urakawa, H., José, R. and Stahl, D.A., 2009. Ammonia oxidation kinetics determine niche separation of nitrifying Archaea and Bacteria. Nature, 461(7266), 976-979.

Matté, S., Botrel, M., Walsh, D.A. and Maranger, R., 2019. Annual nitrification dynamics in a seasonally ice-covered lake. PloS One, 14(3), p.e0213748.

McCarthy, M.J., Lavrentyev, P.J., Yang, L., Zhang, L., Chen, Y., Qin, B. and Gardner, W.S., 2007. Nitrogen dynamics and microbial food web structure during a summer cyanobacterial bloom in a subtropical, shallow, well-mixed, eutrophic lake (Lake Taihu, China). Hydrobiologia, 581, 195-207.

Mulvin, M.R. and Altabet, M.A., 2005. Chemical conversion of nitrate and nitrite to nitrous oxide for nitrogen and oxygen isotopic analysis in freshwater and seawater. Analytical Chemistry, 77(17), 5589-5595.

Newbt, S.N., Stahl, D.A., Casamayor, E.O., Martí, E., Nicol, G.W. and Prosser, J.I., 2012. Differential photoinhibition of bacterial and archaeal ammonia oxidation. FEMS Microbiology Letters, 327(1), 41-46.

Newchamp, M.E., Pick, F.R., Beisner, B.E. and Maranger, R., 2014. Nitrogen forms influence microcystin concentration and composition via changes in cyanobacterial community structure. PloS One, 9(1), p.e85573.

Mukherjee, M., Ray, A., Post, A.F., McKay, R.M. and Bullerjahn, G.S., 2016. Identification, enumeration and diversity of nitrifying planktonic archaea and bacteria in trophic end members of the Laurentian Great Lakes. Journal of Great Lakes Research, 42(1), 39-49.

Newell, S.E., Babbin, A.R., Jayakumar, A. and Ward, B.B., 2011. Ammonia oxidation rates and nitrification in the Arabian Sea. Global Biogeochemical Cycles, 25(4).

Newell, S.E., Davis, T.W., Johengen, T.H., Gossiaux, D., Burtner, A., Palladino, D. and McCarthy, M.J., 2019. Reduced forms of nitrogen are a driver of non-nitrogen-fixing harmful cyanobacterial blooms and toxicity in Lake Erie. Harmful Algae, 81, 86-93.

Nicklisch, A. and Kohl, J.G., 1983. Growth kinetics of Microcystis aeruginosa (Kütz) Kütz as a basis for modelling its population dynamics. Internationale Revue der gesamten Hydrobiologie und Hydrographie, 68(3), 305-326.

Norton, J.M., Klotz, M.G., Stein, L.Y., Arp, D.J., Bottomley, P.J., Chain, P.S., Hauser, L.J., Land, M.L., Larimer, F.W., Shin, M.W. and Starkenburg, S.R., 2008. Complete genome sequence of *Nitrosospira multiformis*, an ammonia-oxidizing bacterium from the soil environment. Applied and environmental microbiology, 74(11), 3559-3572.

Park, H.D., Wells, G.F., Bae, H., Criddle, C.S. and Francis, C.A., 2006. Occurrence of ammonia-oxidizing archaea in wastewater treatment plant bioreactors. Applied and environmental microbiology, 72(8), 5643-5647.

Park, S., Bae, W., Chung, J., & Baek, S. C. (2007). Empirical model of the pH dependence of the maximum specific nitrification rate. Process Biochemistry, 42(12), 1671-1676.

Auer, J.J. and Auer, M.T., 2000. Nitrification in the water column and sediment of a hypereutrophic lake and adjoining river system. Water Research, 34(4), 1247-1254.

Pennsylvania Department of Conservation and Natural Resources (PA DCNR), 2010. http://www.watersheded.dcnr.state.pa.us/training/assignments/dcnr_20031264.pdf

Pester, M., Rattei, T., Flechl, S., Gröngröft, A., Richter, A., Overmann, J., Reinhold-Hurek, B., Loy, A. and Wagner, M., 2012. amoA-based consensus phylogeny of ammonia-oxidizing archaea and deep sequencing of amoA genes from soils of four different geographic regions. Environmental Microbiology, 14(2), 525-539.

Powers, S.M., Baulch, H.M., Hampton, S.E., Labou, S.G., Lottig, N.R. and Stanley, E.H., 2017. Nitrification contributes to winter oxygen depletion in seasonally frozen forested lakes. Biogeochemistry, 136, 119-129.

Prosser, J.I., 1990. Autotrophic nitrification in bacteria. In *Advances in Microbial Physiology* (Vol. 30, 125-181). Academic Press.

R Core Team (2022). R: A language and environment for statistical computing. R Foundation for Statistical Computing, Vienna, Austria. URL: https://www.R-project.org/.

Reed, M.H., Strope, E.K., Cremona, F., Myers, J.A., Newell, S.E. and McCarthy, M.J., 2023. Effects of filtration timing and pore size on measured nutrient concentrations in environmental water samples. Limnology and Oceanography: Methods, 21(1), 1-12.

Ripley, B., Venables, B., Bates, D.M., Hornik, K., Gebhardt, A., Firth, D. and Ripley, M.B., 2013. Package 'mass'. Cran R, 538.

Saarenheimo, A.J., Tiirola, M., Hietanen, S. and Ojala, A., 2013. Interlake variation and environmental controls of denitrification across different geographical scales. Aquatic Microbial Ecology, 69(1), 1-16.

Rotthauwe, J.H., Witzel, K.P. and Liesack, W., 1997. The ammonia monooxygenase structural gene amoA as a functional marker: molecular fine-scale analysis of natural ammonia-oxidizing populations. Applied and Environmental Microbiology, 63(12), 4704-4712.

Scavia, D., Allan, J.D., Arend, K.K., Bartell, S., Beletsky, D., Bosch, N.S., Brandt, S.B., Briland, R.D., Daloğlu, I., DePinto, J.V. and Dolan, D.M., 2014. Assessing and addressing the re-eutrophication of Lake Erie: Central basin hypoxia. Journal of Great Lakes Research, 40(2), 226-246.

Stumpf, R.P., Wynne, T.T., Baker, D.B. and Fahnenstiel, G.L., 2012. Interannual variability of cyanobacterial blooms in Lake Erie. PloS one, 7(8), p.e42444.

Tavia, D., Wang, Y.C. and Obenour, D.R., 2023. Advancing freshwater ecological forecasts: Harmful algal blooms in Lake Erie. Science of The Total Environment, 856, p.158959.

Tsimmas, N.K., 1986. Interactions of temperature, pH, and biomass on the nitrification process. Water Pollution Control Federation, 52-59.

Veall, G.E., Bullerjahn, G.S., Sterner, R.W., Beall, B.F., Brovold, S., Finlay, J.C., McKay, R.M. and Mukherjee, M., 2013. Rates and controls of nitrification in a large oligotrophic lake. Limnology and Oceanography, 58(1), 276-286.

Veall, G.E., Cotner, J.B., Finlay, J.C., Stark, R.A. and Sterner, R.W., 2014. Nitrogen transformations at the sediment–water interface across redox gradients in the Laurentian Great Lakes. Hydrobiologia, 731(1), 95-108.

Veall, G.E., Finlay, J.C., McKay, R.M.L., Rozmarynowycz, M.J., Brovold, S., Bullerjahn, G.S., Spokas, K. and Sterner, R.W., 2016. Large differences in potential denitrification and sediment microbial communities across the Laurentian great lakes. Biogeochemistry, 128, 353-368.

Veffen, M.M., Li, Z., Effler, T.C., Hauser, L.J., Boyer, G.L. and Wilhelm, S.W., 2012. Comparative metagenomics of toxic freshwater cyanobacteria bloom communities on two continents. PloS one, 7(8), p.e44002.

Vi, Q., Schittich, A. R., Jensen, M. M., Ng, H., & Smets, B. F. (2021). Role of ammonia oxidation in organic micropollutant transformation during wastewater treatment: insights from molecular, cellular, and community level observations. Environmental Science & Technology, 55(4), 2173-2188.

Wasamura, N., Iwakuma, T. and Yasuno, M., 1987. Uptake of 13C and 15N (ammonium, nitrate and urea) by Microcystis in Lake Kasumigaura. Journal of Plankton Research, 9(1), 151-165.

United States Environmental Protection Agency. https://www.epa.gov/greatlakes/physical-features-great-lakes. Accessed 2019-10-21.

Vanderploeg, H.A., Liebig, J.R., Carmichael, W.W., Agy, M.A., Johengen, T.H., Fahnenstiel, G.L. and Nalepa, T.F., 2001. Zebra mussel (Dreissena polymorpha) selective filtration promoted toxic Microcystis blooms in Saginaw Bay (Lake Huron) and Lake Erie. Canadian Journal of Fisheries and Aquatic Sciences, 58(6), 1208-1221.

Wagner, M., Rath, G., Amann, R., Koops, H.P. and Schleifer, K.H., 1995. In situ identification of ammonia-oxidizing bacteria. Systematic and Applied Microbiology, 18(2), 251-264.

Wang, X., Depew, D., Schiff, S. and Smith, R.E., 2008. Photosynthesis, respiration, and stable isotopes of oxygen in a large oligotrophic lake (Lake Erie, USA–Canada). Canadian Journal of Fisheries and Aquatic Sciences, 65(11), 2320-2331.

Ward, B.B., 2008. Nitrification in marine systems. *Nitrogen in the Marine Environment*, *2*, 199-261.

Watson, S.B., Miller, C., Arhonditsis, G., Boyer, G.L., Carmichael, W., Charlton, M.N., Confesor, R., Depew, D.C., Höök, T.O., Ludsin, S.A. and Matisoff, G., 2016. The re-eutrophication of Lake Erie: Harmful algal blooms and hypoxia. Harmful Algae, 56, 44-66.

Y., Lu, J., Wang, Y., Liu, G., Wan, X., Hua, Y., ... & Zhao, J. (2020). Diversity and abundance of comammox bacteria in the sediments of an urban lake. Journal of Applied Microbiology, 128(6), 1647-1657.

Yang, J., Gao, H., Glibert, P.M., Wang, Y. and Tong, M., 2017. Rates of nitrogen uptake by cyanobacterially-dominated assemblages in Lake Taihu, China, during late summer. Harmful Algae, 65, 71-84.

Yang, Y., Li, N., Zhao, Q., Yang, M., Wu, Z., Xie, S., & Liu, Y. (2016). Ammonia-oxidizing archaea and bacteria in water columns and sediments of a highly eutrophic plateau freshwater lake. Environmental Science and Pollution Research, 23, 15358-15369.

Yang, Y., Daims, H., Liu, Y., Herbold, C. W., Pjevac, P., Lin, J. G., ... & Gu, J. D. (2020). Activity and metabolic versatility of complete ammonia oxidizers in full-scale wastewater treatment systems. Mbio, 11(2), 10-1128.

Zastepa, A., Comte, J. and Crevecoeur, S., 2023a. Prevalence and ecological features of deep chlorophyll layers in Lake of the Woods, a complex hydrological system with strong trophic, physical, and chemical gradients. Journal of Great Lakes Research, 49(1), 122-133.

Zastepa, A., Westrick, J. A., Liang, A., Birbeck, J. A., Furr, E., Watson, L. C., ... & Crevecoeur, S., 2023b. Broad screening of toxic and bioactive metabolites in cyanobacterial and harmful algal blooms in Lake of the Woods (Canada and USA), 2016–2019. *Journal of Great Lakes Research*, *49*(1), 134-146.

Zeng, J., Zhao, D.Y., Huang, R. and Wu, Q.L., 2012. Abundance and community composition of ammonia-oxidizing archaea and bacteria in two different zones of Lake Taihu. Canadian Journal of Microbiology, 58(8), 1018-1026.

Zhang, Y., Chen, L., Sun, R., Dai, T., Tian, J. and Wen, D., 2015. Ammonia-oxidizing bacteria and archaea in wastewater treatment plant sludge and nearby coastal sediment in an industrial area in China. Applied Microbiology and Biotechnology, 99(10), 4495-4507.